

10 NOV. 1970



ICAS Paper No. 70-06

**COMPARISON OF HEAT TRANSFER MEASUREMENTS
IN FREE FLIGHT AND IN A WIND TUNNEL AT M=7 AT
SIMILAR REYNOLDS NUMBERS AND TEMPERATURE RATIOS**

m. h. by

Bo Lemcke, Aeronautical Research Institute of Sweden,
A. Naysmith and John Picken, RAE Farnborough, U.K.
H. Thomann, ETH Zurich, Switzerland

The Seventh Congress of the International Council of the Aeronautical Sciences

CONSIGLIO NAZIONALE DELLE RICERCHE, ROMA, ITALY / SEPTEMBER 14-18, 1970

Price: 400 Lire

BT

COMPARISON OF HEAT TRANSFER MEASUREMENTS IN FREE FLIGHT
AND IN A WIND TUNNEL AT $M = 7$ AT SIMILAR REYNOLDS NUMBERS
AND TEMPERATURE RATIOS.

Bo Lemcke*, Alan Naysmith**, John Picken**, Hans Thomann***,

Abstract

A free flight model (a paraboloid of revolution) was designed and built at the Royal Aircraft Establishment in England. Prior to the flight from the Woomera range in Australia it was tested in the hypersonic tunnel Hyp 500 at the Aeronautical Research Institute of Sweden. At $M = 7.17$ it was possible to simulate Reynolds number and cooling ratio. As the same model and the same instrumentation was used in both cases, nearly perfect aerodynamic simulation was possible.

The heat transfer results from the two experiments are in close agreement and agree well with theoretical predictions for laminar and turbulent boundary layers.

The transition Reynolds number in flight was lower than in the wind tunnel. There are indications that vibrations from the rocket motor affected transition in flight.

The transition Reynolds number varied during flight in a way that suggests that the boundary layer was affected considerably by changes in angle of incidence. No comparable effect was detected during the wind tunnel tests.

1. Introduction

For many years, free flight measurements of heat transfer and pressure distribution have been conducted by the Royal Aircraft Establishment (RAE), in Farnborough. In the spring of 1965 it was observed that the hypersonic wind tunnel Hyp 500 at the Aeronautical Research Institute of Sweden (FFA) could almost perfectly simulate the free flight conditions which RAE's hypersonic test vehicle, Jabiru, encountered at $M = 4$ and 7. The following cooperation was therefore initiated:

- i. Models should be designed, built and instrumented at the RAE.
- ii. These models should then be sent to FFA where they would be tested in the tunnel Hyp 500. In this test, Mach number M , Reynolds number Re and the ratio of wall temperature

to free stream temperature T_w/T_∞ expected in the flight would be simulated as closely as possible and heat transfer and pressure distribution would be measured.

- iii. The model would then be sent back to RAE to be fitted to the test vehicle and flight tested on the range at Woomera.

For the first test of this series a simple shape (paraboloid) was chosen (see Figs. 1 and 2).

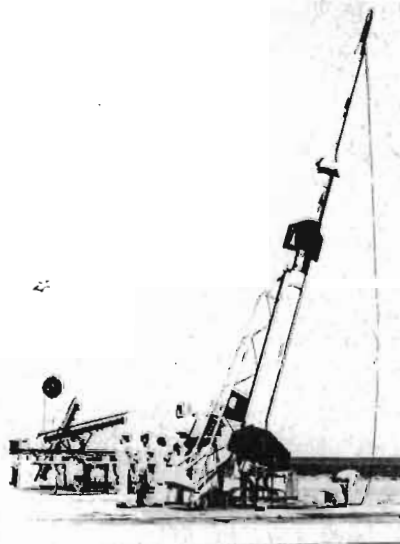


Figure 1. Picture of the model on the test vehicle

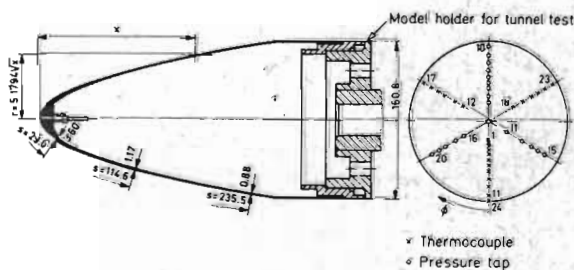


Figure 2. Shape of model and location of thermocouples and pressure taps. All lengths in mm.

* Aero. Res. Institute of Sweden (FFA)

** Royal Aircraft Establishment, Farnborough, UK (RAE)

*** ETH Zürich, Switzerland

The distribution of wall thickness along the generator was designed to give uniform wall temperature for the whole part of the model covered with a laminar boundary layer. The purpose of the experiment was twofold. First, reliable experimental results for heat transfer and pressure distribution on a blunt shape should be generated to check existing methods of calculation. Second, to use the perfect simulation possible (equal M , Re , T_w/T_∞ and identical model) to check the experimental accuracy of the two tests, especially of the influence of transition.

The tests in the wind tunnel are described in detail by Thomann (1). After these tests, the model was fired from the Woomera range in Australia. A detailed description of the vehicle, the calibration and the data transmission is given by Picken (2). The flight and the data reduction are described by Naysmith in (3). An independent reduction of the flight data was conducted by Lemcke at PFA. In the present paper the essential part of this work is collected and the results are compared. Good agreement between the experiments and between the experiment and the theories used for comparison of the heat transfer data (4), (5) were found. Unexpected was the observation that transition in flight occurred at a lower Reynolds number than in the tunnel. There are strong indications that this was caused by motor induced vibrations.

Only a few published comparisons between tunnel tests and free flight heat transfer data are known to the author. In his survey paper, Poisson-Quinton (6) gives an example of excellent agreement of both heat transfer and transition at $M = 2$. The second example he quotes stems from the French Berenice project. Good agreement for a laminar boundary layer on a re-entry body at $M = 10$ was found. In (7) results of the X-15 project are shown.

2. Model and instrumentation

(common to both tests)

The model was a paraboloid of revolution (Fig. 2) 240.8 mm long followed by a short cylindrical section terminating in a circular base. The shape was generated by rotating the curve $r = 5.1794 \sqrt{x}$ (dimension in mm) about the x axis. The model was machined from solid inconel and the wall thickness varied from 4.43 mm at the station of the first thermocouple near the nose to 0.88 mm near the base. The distribution of thickness was designed - using approximations that in the event proved to be less accurate than had been anticipated - to give a uniform temperature in laminar flow at a representative Mach number.

A highly polished radiation shield of chromium-plated mild steel was fitted inside the model about 6 mm from the wall. It suppressed internal heat transfer by radiation.

The model was instrumented with 25 chromel-alumel thermocouples arranged along three generators symmetrically disposed round the model ($\theta = 0, 120^\circ$ and 240°) as shown in Fig. 2. The wires, which had a diameter of 0.1 mm, were individually spot-welded to the inside of the model wall at points approximately 0.25 mm apart.

The surface pressure orifices had a diameter of 1.05 mm. They were connected with copper tubing, of internal diameter 1.75 mm, to the pressure transducers.

3. Free flight test.

The Jaribu MK.2 is a three-stage hypersonic rocket vehicle. It was fired from the Woomera range in Australia. Approximately 18 seconds after launch the model, still attached to the third stage of the rocket, attained a Mach number of 8.61. Radio Doppler measurements and kinetheodolite records were used to determine the trajectory. Combined with meteorological data (pressure, temperature and wind speed) from meteorological balloons and standard radiosonde equipment, the information needed to reduce the heat transfer measurements ("still air velocity" U_∞ , T_∞ and p_∞) was obtained. This information is shown in Figs. 3 and 4.

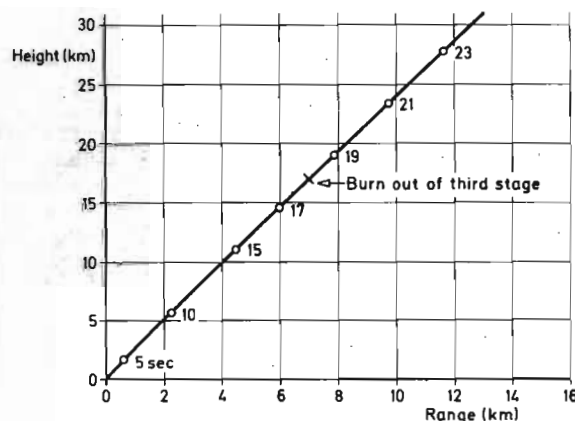


Figure 3. Trajectory of the flight.

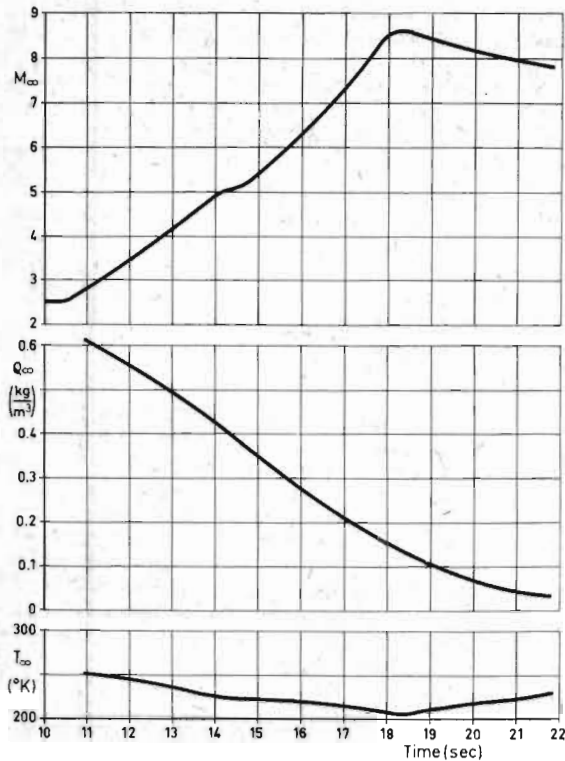


Figure 4. Free stream conditions as function of flight time

A high speed multiplexer connected to standard telemetry equipment was used to transmit the output of 18 thermocouples to the ground. These thermocouple outputs (3-11, 13 - 17 and 19 - 22 on Fig. 2) were recorded every 0.0106 seconds. Of the remaining thermocouples two (2 and 12) were sampled every 0.127 seconds and the rest every 0.254 seconds.

Variable inductance pressure transducers were used to measure the pressures. Their output was telemetered to the ground via a multiplexer, sampling some of the outputs every 0.25 seconds, some every 0.12 seconds.

Further instruments used were 4 accelerometers for longitudinal and lateral accelerations, a magnetometer for measuring the rate of roll, and a thermistor embedded in the thermocouple cold junction tray.

All airborne telemetry signals were received on the ground and recorded on magnetic tape in analogue form.

Information about the accuracy of the whole system is gained by comparing the measured and transmitted pressure at the stagnation

point of the vehicle with the value calculated from the flight velocity and the atmospheric data. During the whole flight, the difference was less than 2% and at $M = 7.17$ it was about 1%.

4. Wind tunnel tests

Before the flight the model was tested in the hypersonic tunnel Hyp 500 at FFA at $M = 7.17$. The tunnel is of blowdown type with a test section diameter of 500 mm, a stagnation pressure of about 100 bar and a stagnation temperature of about 700°K. This resulted in a Reynolds number $\rho_{\infty} U_{\infty} D / \mu_{\infty} = 5 \cdot 10^6$, which is essentially the value attained in free flight. The Mach number distribution in the test section is shown in Fig.5.

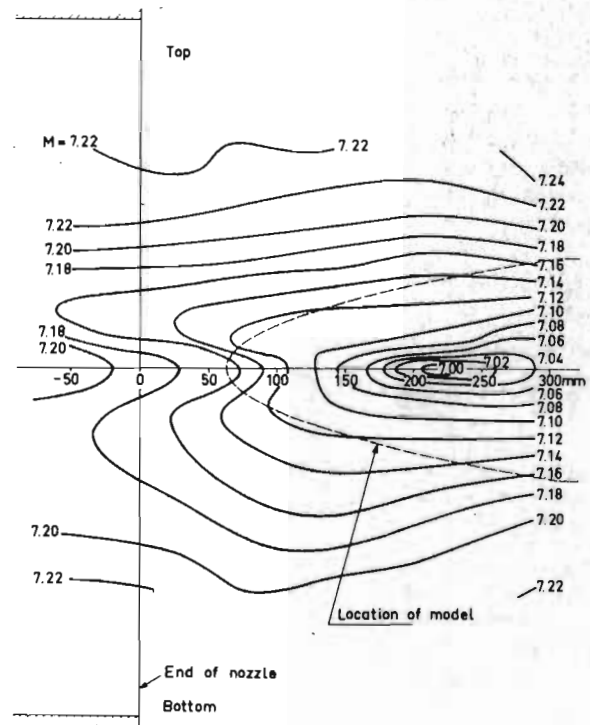


Figure 5. Mach number distribution in the test section of the wind tunnel

The model was mounted on an injection device which moved it into the established flow field in the test section. This resulted in very good initial conditions for the heat transfer measurements. In order to simulate the correct ratio of wall temperature to free stream temperature, the model could be precooled with solid CO_2 to about 200°K. Full details of the experiments are given in (1).

5. Data reduction

The temperature measurements were reduced to heat transfer rates and are presented in the following way.

$$St = \frac{q}{\rho_{\infty} U_{\infty} (h_r - h_w)} \quad (1)$$

Here ρ_{∞} and U_{∞} are the density and the velocity in front of the shock wave and h_w is the enthalpy of the air at surface temperature and pressure. The recovery enthalpy h_r was calculated from

$$h_r = h_e + r (h_o - h_e)$$

with $r = 0.842$ for laminar flow and $r = 0.9$ for turbulent flow. The stagnation enthalpy h_o and the enthalpy h_e at the outer edge of the boundary layer were calculated from T_{∞} , U_{∞} and the measured wall pressures assuming that the entropy at the outer edge of the boundary layer was equal to the entropy behind a normal shock. Real air properties were taken from (8).

Surface temperature and heat transfer rate were deduced from the measured backface temperature T using the following expressions

$$T_w(t) = T(t) + \frac{\rho c d^2}{2k} \frac{dT}{dt} + \frac{\rho^2 c^2 d^4}{24k^2} \frac{d^2T}{dt^2} + \dots \quad (2)$$

$$\bar{q}(t) = \rho c d \frac{dT}{dt} + \frac{\rho^2 c^2 d^3}{6k} \frac{d^2T}{dt^2} + \frac{\rho^3 c^3 d^5}{120k^2} \frac{d^3T}{dt^3} + \dots \quad (3)$$

which are based on the assumption that the properties of the material (ρ, c, k) are constant across the wall and that the backface of the wall is insulated. The \bar{q} from Eq.(3) were corrected for conduction effects (at RAE only) and for radiation losses to space. Internal heat transfer by radiation was prevented by the radiation shield.

At this point, however, the idea of perfect simulation of the flight in the tunnel comes to its end, as in flight the q is about 10 times the \bar{q} in the tunnel. The heat conduction in the wall is therefore no longer similar. In the tunnel test the temperature across the wall was essentially uniform and therefore, only the first terms in Eqs.2 and 3 were needed. In flight, however, the difference between the surface temperature and the inside temperature was as high as 100°C and could no longer be neglected. Therefore, three terms had to be taken into account in Eqs.2 and 3.

The time derivatives were determined in different ways. At RAE a least squares third degree polynomial was fitted through 171 points, covering 1.8 sec of the real

flight time. All derivatives were determined in the middle of the interval.

At FFA a straight line was fitted through 70 points covering an interval of 0.74 sec. From this dT/dt was determined. Through these dT/dt another straight line was fitted and d^2T/dt^2 was determined from this. The third derivative was determined in the same way.

For the tunnel test, straight lines through 5 or 11 points were used giving essentially the same results, but with increased scatter for the 5 point data.

These methods have the drawback that the past history and the future have the same influence on the slope in the middle of the interval, whereas physically only the past counts. Just before transition occurs a slope somewhere between laminar and turbulent is therefore determined, instead of the laminar one. This was the case for $M = 4.17$ (Fig.7). These data were therefore reduced with a method developed by Lemcke which takes into account only the past.

6. Results, comparison with theory

Heat transfer

The measured Stanton numbers and the wall temperatures $T_w(s)$ for $\theta = 0^\circ$ are plotted in Figs. 6 to 11 for Mach numbers from 3.57 to 8.17. Also indicated were the real-gas stagnation temperatures T_o , as the variations in wall temperature should be compared with $T_o - T_w$. For lower Mach numbers the data reduction was difficult because of the small difference between T_o and T_w . In Figs.12 and 13 the results of the tunnel test at $M = 7.17$ are shown. These results are compared with theoretical prediction for laminar and turbulent boundary layers.

For the laminar case the convenient method suggested by Crabtree et.al. (4) was used. It is based on Eckert's reference enthalpy

$$h^* = 0.5 (h_w + h_e) + 0.22 (h_r - h_e) \quad (4)$$

and an equivalent flat-plate length X connected with the physical length s along the surface by

$$X = \frac{\int_0^s \rho^* \mu^* U_e r^2 ds}{\rho^* \mu^* U_e r^2} \quad (5)$$

with $\rho^* = \rho(h^*, p_e)$ and $\mu^* = \mu(h^*)$

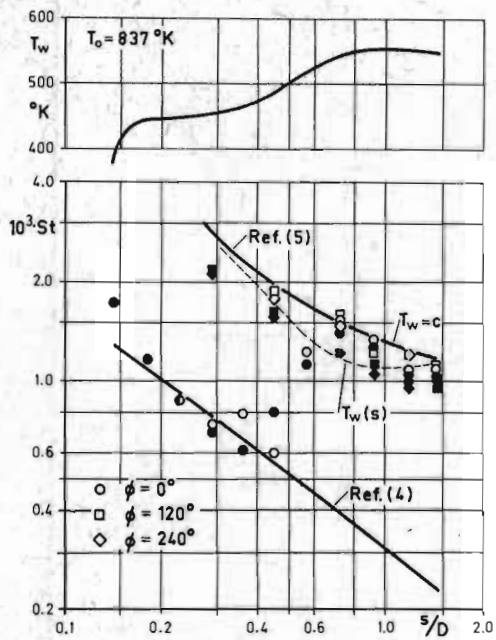


Figure 6. Stanton numbers and wall temperature
Flight test at $M=3.57, Re = 6.24 \cdot 10^6$

○ □ ◇ Data reduced at FFA
● ■ ◆ Data reduced at RAE

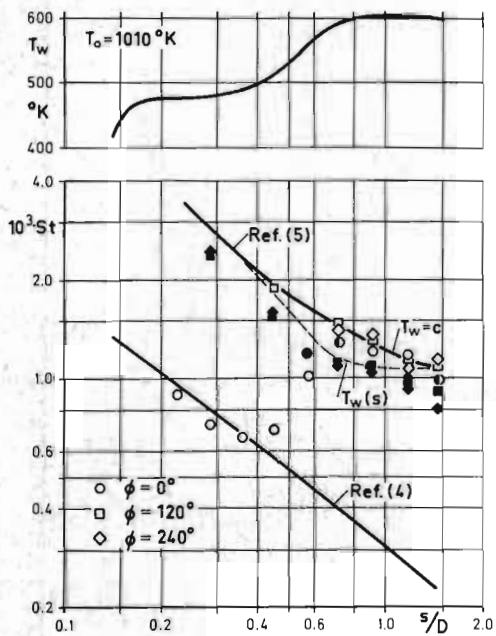


Figure 7. Stanton numbers and wall temperature.
Flight test at $M=4.17, Re = 6.63 \cdot 10^6$

○ □ ◇ Data reduced at FFA
● ■ ◆ Data reduced at RAE

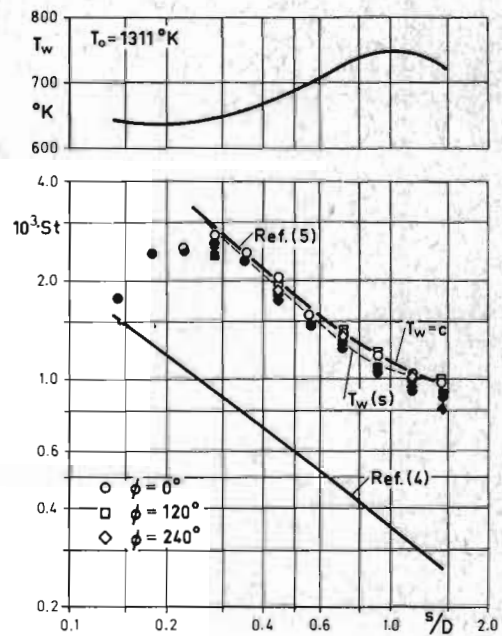


Figure 8. Stanton numbers and wall temperature.
Flight test at $M=5.17, Re = 6.38 \cdot 10^6$

○ □ ◇ Data reduced at FFA
● ■ ◆ Data reduced at RAE

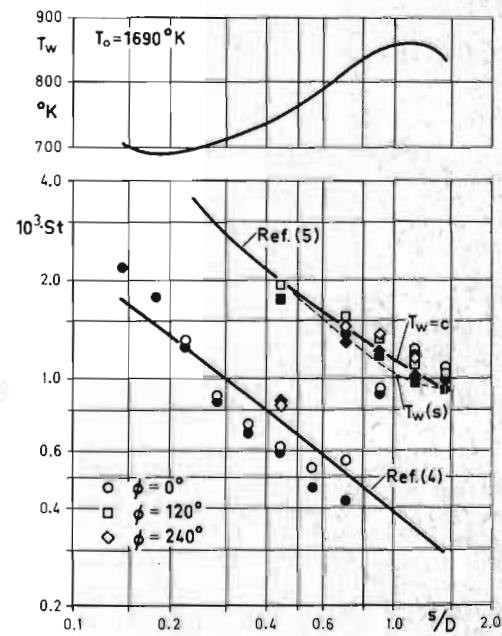


Figure 9. Stanton numbers and wall temperature.
Flight test at $M=6.17, Re = 5.92 \cdot 10^6$

○ □ ◇ Data reduced at FFA
● ■ ◆ Data reduced at RAE

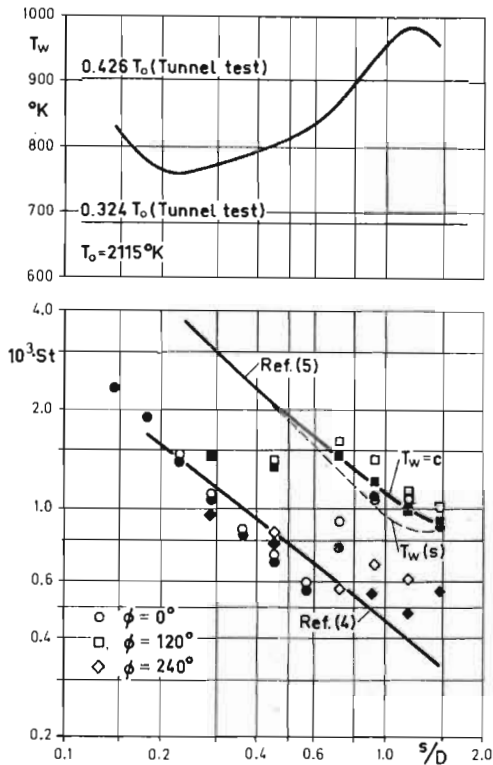


Figure 10. Stanton numbers and wall temperature.
Flight test at $M = 7.17$, $Re = 5.32 \cdot 10^6$

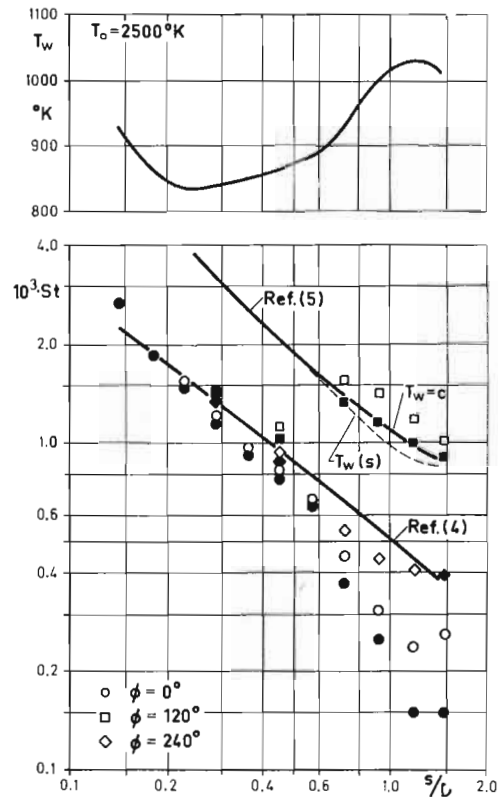


Figure 11. Stanton numbers and wall temperature.
Flight test at $M = 8.17$, $Re = 4.78 \cdot 10^6$

The effect of the pressure gradient is taken into account with a factor a defined as

$$a = 0,332 \left[1 + 0,1853 \sqrt{\frac{2 X}{U_e} \frac{dU_e}{ds}} \right] \quad (6)$$

With these expressions, the heat transfer rate q becomes

$$q = a \cdot \sqrt{\frac{\rho^* \mu^* U_e}{X}} \cdot Pr^{*-2/3} (h_r - h_w) \quad (7)$$

Good agreement between theory and experiment is found as can be seen in Figs. 6 to 11 for the flight test. The same is true for the tunnel test (Fig.12). The difference between the theoretical predictions for flight and tunnel is mainly due to the different temperature levels of the tests. In flight at $M = 7.17$ the reference temperature T^* was around 1300°K and in the tunnel it was around 400°K.

For the turbulent case, a computer program based on a method suggested by Walz (Rechenmethode II + Chapter 5.2. and 5.3 in (5)), was used. It is based on integral equations

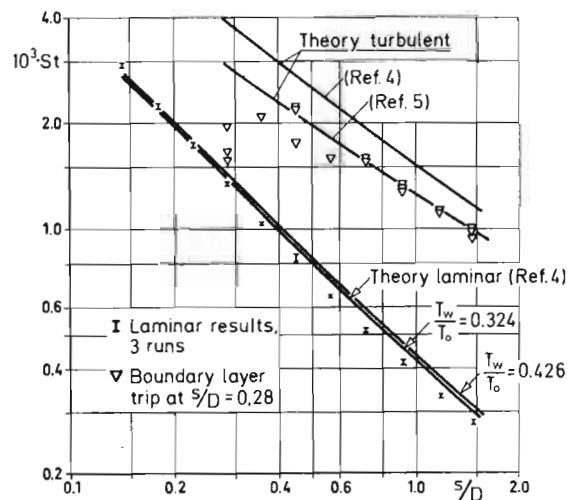


Figure 12. Stanton numbers. Tunnel test at $M = 7.17$, $Re = 5.10^6$. No angle of attack

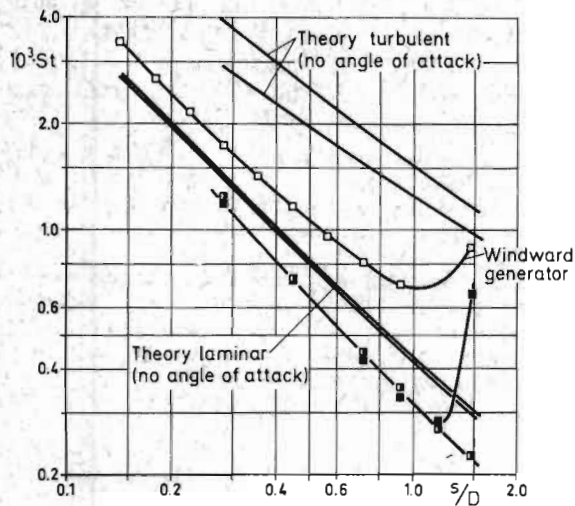


Figure 13. Stanton numbers, Tunnel test at $M = 7.17$, $Re = 5.10^6$, 5° angle of attack

for momentum, energy and mechanical energy and takes into account the variation with s of T_w . As the prediction of the latter effect is not too well supported by experiments, results for $T_w(s) = \text{const.}$ as well as for the actual distribution $T_w(s)$ are included in Figs. 6 - 11. It is seen that the uncertainty introduced by the nonuniform surface temperature is small. Also in this case the agreement between experiments and theory is good.

Pressure distribution

In Fig. 14 the pressure distributions at $M = 7.17$ in flight and in the tunnel are compared. The pressures are shown relative to the values predicted with the modified Newton theory. Both experiments are close to this simple theory, the tunnel results being somewhat higher, probably due to the variation in free stream Mach number shown in Fig. 5.

Transition

From the heat transfer measurements the location of transition was determined. In the wind tunnel test a small surface irregularity (3 mm long, 1 mm wide and about 0.1 mm high) was present in front of the generator containing the thermocouples 12 to 17. With the uncooled model ($T_w/T_o = 0.426$) the flow on generators 1 to 11 and 18 to 23 was completely laminar. After removing the irregu-

larity, the onset of transition on generator 12 to 17 moved from $s/D = 0.4$ to $s/D = 0.9$. With the cooled model ($T_w/T_o = 0.324$) only the generator 1 to 11 was fully laminar. On the other two generators transition started at about $s/D = 0.3$ and 0.4. No tests without surface irregularity were made. At 5° angle of attack transition was close to the end of the model as can be seen from Fig. 13 (no surface irregularity).

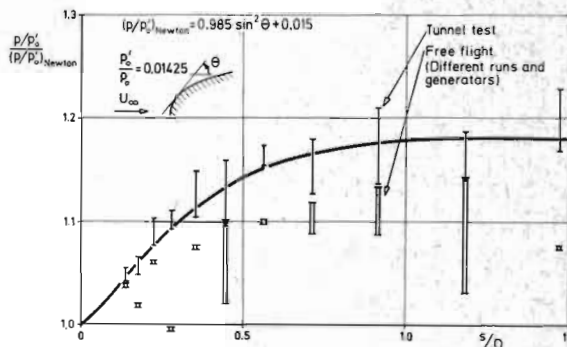


Figure 14. Normalized pressure distribution, flight and tunnel test at $M = 7.17$

For the free flight test, results were quite different. Large parts of the model were covered with a transitional or turbulent boundary layer, as can be seen in Fig. 15. It is believed that the early transition is caused by motor-induced vibrations or by an angle of attack of the vehicle.

The first cause was investigated in the following way. Between the burnout of the second stage and the ignition of the third stage there is an interval of about 0.2 sec with reduced vibrations during which the boundary layer, according to the hypothesis, should be laminar. Therefore, straight lines were fitted through the temperatures and extrapolated to the center of the interval. If the flow remains turbulent through-out the lines should intersect at a shallow angle, if the flow is turbulent before and after but laminar in the interval, the line at the later time should be approximately parallel to the earlier line but at a lower temperature as indicated in Fig. 16.

It can be seen that the agreement is as good as can be expected, especially if the uncertainty in the length of the interval with laminar flow is taken into account. The small ΔT for $s/D \geq 1$ can be explained by assuming that natural transition without

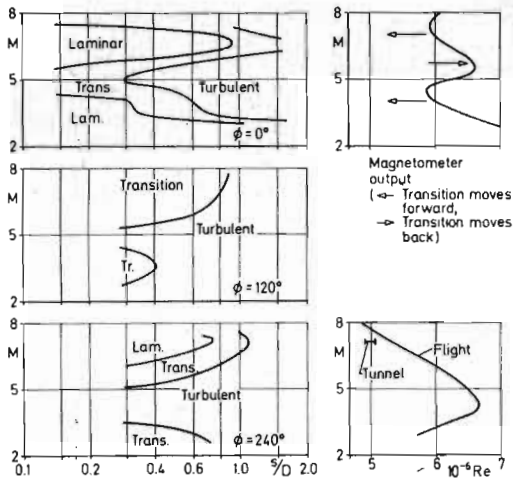


Figure 15. Location of transition as function of Mach number, compared with magnetometer output.

vibrations is present in this range, which is an agreement with the tunnel tests.

The accelerations of the vehicle normal to the axis of symmetry were measured. 90% of the readings were in a band of ± 0.4 g with a predominant frequency of about 5 cps. This is mentioned to give some indication of the type of vibrations present.

As can be seen in Fig. 15 the rolling motion of the vehicle relative to the magnetic field of the earth is correlated with the motion of transition on the model surface. This suggests an angle of attack effect. However, this is contradicted by the fact that 5° angle of attack in the tunnel had a small influence on transition (Fig. 13) while the angle of attack in flight was below 1° (from pressure measurement).

7. Conclusions

In the present case of nearly "perfect aerodynamic simulation" of the flight in a wind tunnel, good agreement for laminar and turbulent heat transfer rates was found.

Perfect simulation is not possible, as the conduction in the wall was different for the two cases (much higher q during the flight) and as air is not an ideal gas in the whole temperature range. Both effects can be taken into account theoretically.

In flight transition occurred at a lower Reynolds Number than in the tunnel. It is likely that motor-induced vibrations are the cause but some indications exist that a small angle of attack had some influence.

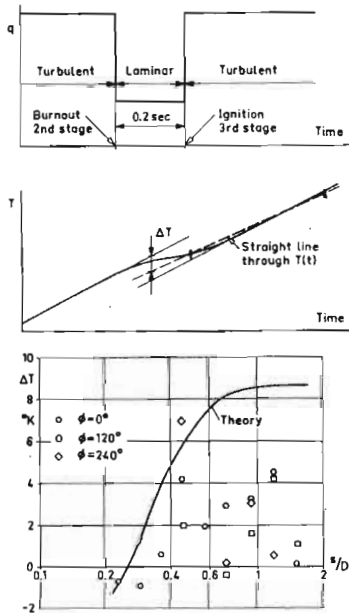


Figure 16: Method used to investigate the influence of vibration on transition at $M = 5.05$

References

1. Thomann, H.: Heat transfer Measurements at $M = 7.17$.
-First step of a comparison between tunnel test and free flight
FFA, Report 110 (1967)
2. Picken, J.: Final Specification of the free flight vehicle Jabiru UK/E
Tech Memo Aero 1051 (1968)
3. Naysmith, A.: Measurements of heat transfer rates and boundary layer transition on a blunt nosed body of revolution in free flight at supersonic and hypersonic speeds.
RAE, TR No. 70096
4. Crabtree, L.F., Dommett, R.L., Woodley, J.G., Estimation of heat transfer to flat plates, cones and blunt bodies
RAE TR No. 65137 (1965)
5. Walz, A.: Strömungs-und Temperatur - grenzschichten (Karlsruhe 1966)
6. Poisson-Quinton, Ph.: From wind tunnel to flight, the role of the laboratory in Aerospace design.
J. of Aircraft, Vol.5, No.3 (1968)
7. Toll, T.A., Fischel, J.: The X-15 project: results and new research. Astronautics and Aeronautics (March 1964)
8. Hilsenrath, J. et al: Tables of thermodynamic and transport properties of air, argon, carbon dioxide, carbon monoxide, hydrogen, nitrogen, oxygen, and steam (Oxford 1960)
9. Trimpi, R.L., Jones, R.A.: Transient temperature distribution in a two-component semi-infinite composite slab of arbitrary materials subjected to aerodynamic heating with a discontinuous change in equilibrium temperature or heat-transfer coefficient. NACA, TN 4308 (1958)